Materials Research Proceedings 28 (2023) 1295-1302 https://doi.org/10.21741/9781644902479-140

Cutting force in peripheral milling of cold work tool steel

TAMURA Shoichi [1,a *] and MATSUMURA Takashi [2,b]

[1]Ashikaga University, 268-1 Omae-cho, Ashikaga-shi, Tochigi, 326-8558, Japan

[2]Tokyo Denki University, 5 Senjyu Asahi-cho, Adachi-ku, Tokyo, 120-8551, Japan

[a]tamura.shoichi@g.ashikaga.ac.jp, [b]tmatsumu@cck.dendai.ac.jp

Keywords: Cutting Force, Residual Stress, Surface Finish, Heat Treatment

Abstract. Tool steels have been commonly applied to die and mold parts because of the high strength and the high abrasive wear resistance obtained by the heat treatments. In order to achieve high machining rate, the heat-treated tool steels have recently finished with end mills coated by hard thin layers. The cutting force in milling of the tool steel should be controlled to improve the fatigue lives of die and mold, which are associated with not only the surface qualities but also the microstructure in the subsurface. This paper discusses the cutting process in milling of a cold work tool steel in terms of the cutting force and the residual stress in finished subsurface.

Introduction

Tool steels have been applied to die and mold manufacturing due to their excellent mechanical strengths, and wear resistances. Milling of tool steel has been usually performed before quenching of workpiece, then the hardened product has been finished in polishing so far. Because hard milling without polishing is required to improve productivity and product quality, advanced cutting tool and coating materials, such as gradient cemented carbide with different grain sizes, has been developed [1].

Durakbasa et al. [2] performed milling of AISI H13 hot work tool steel to optimize end cutting parameters by Taguchi method. The authors summarized that an end mill coated with AlTiN showed better performance regarding the surface finish and the tool wear resistance in comparison to TiAlCN and ZrN coatings. Aramcharoen et al. investigated the effects of coating materials in milling of hardened tool steel H13 with a 0.5 mm diameter micro end mill [3]. They concluded TiN coated tool was effective to control the tool wear, the chipping, the surface finish, and the burr formation.

Furthermore, the die and molding manufacturing has recently required for control of the affected layer and the residual stress in subsurface in terms of lives of die and mold. Denkena et al. conducted hard millings for AISI H13 [4]. They reported that the undercut geometry of the flank face reduced the tensile residual stress and the tool wear. Caruso et al. investigated the residual stress in subsurface in dry orthogonal cutting of AISI 52100 steel [5]. The large compressive residual stress was obtained in cutting of a harder workpiece with a chamfered tool. Although a large number of experiments have been conducted to investigate the cutting characteristics of tool steels so far, the analytical works have not yet been done so much to discuss the cutting process of hardened tool steels in terms of the properties of surface and subsurface.

The paper studies the cutting process in peripheral milling of a hardened cold tool steel comparing with a carbon steel. The cutting tests are conducted to measure the cutting force and the residual stresses and observe the surface finish. The cutting processes, then, are discussed in an analytical force model. The residual stress in subsurface was associated with the shear plane cutting model.

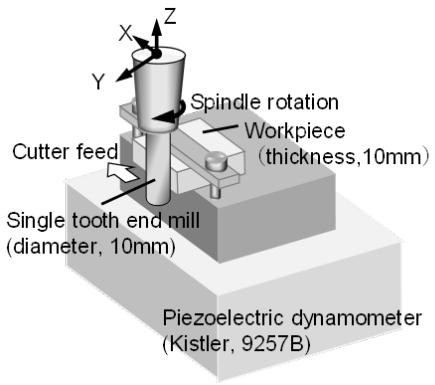

Fig. 1 Cutting test in peripheral milling.

Table 1 Cutting conditions.

Axial depth of cut [mm]	10
Radial depth of cut [mm]	0.1
Cutting speed [m/min]	25
Feed rate [mm/tooth]	0.05
Cutting direction	Down-cut
Lubrication	Dry

Cutting Test

The cutting tests in peripheral milling were conducted on a 3-axis machining center (FANUC Robodrill α-T14iF), as shown in Fig. 1. A 10 mm thick plate of tool steel (JIS, SKD11) was employed as a workpiece for the cutting test. The workpiece was quenched and tempered at 1020℃ and 220℃ in a vacuum furnace, and controlled the hardness of 54 HRC before the cutting test. In addition, a plate of carbon steel (JIS, S50C) with a controlled hardness of 14 HRC was also used as a reference. The workpiece was clamped on a piezoelectric dynamometer (Kistler, 9257B) mounted on the machine table to measure the cutting force. A single tooth square end mill coated with AlCN thin layer, which was ground off one tooth from the original two teeth end mill, was employed to exclude the influence of the cutter runout. The tool diameter and the helix angle were 10 mm and 30°, respectively. The end mill was clamped to the spindle of the machine tool with a collet chuck. The reference surface was machined to control the radial depth of cut before the cutting test. The end mill was fed along +X direction in down-cut peripheral milling at an axial depth of cut of 10 mm, and a radial depth of cut of 0.1 mm, as shown in Table 1. In order to reduce the vibration occurring in the initial cutting state with the sharp edge, the flank wear land was control so as to contact the workpiece in a width of approximately 20 μm by preliminary cutting, where the cutting speed, the feed rate, and the feed travel were 25 m/min, 0.1 mm/tooth, and 30 mm, respectively. The low cutting speed for milling of steel was set to reduce tool vibration, even though the cutting speed was possibly associated with the surface finish. Then, the residual stresses of the machined surfaces were measured in the feed direction (X-axis) and the axial direction (Z-axis) to compare with the residual stress measured before machining, where the machined surfaces were not processed for the measurements. The residual stresses were measured with an X-ray residual stress analyzer (Pulstec, μ-X360s) based on the cos α method [6]. The measurements for each workpiece were conducted at three points on the center line of workpiece thickness.

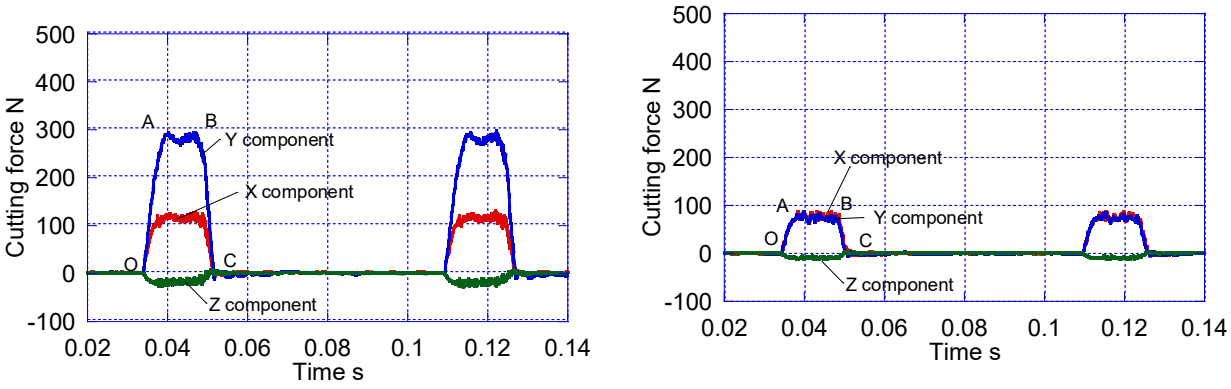

(a) Tool steel (b) Carbon steel

Fig. 2 Cutting forces.

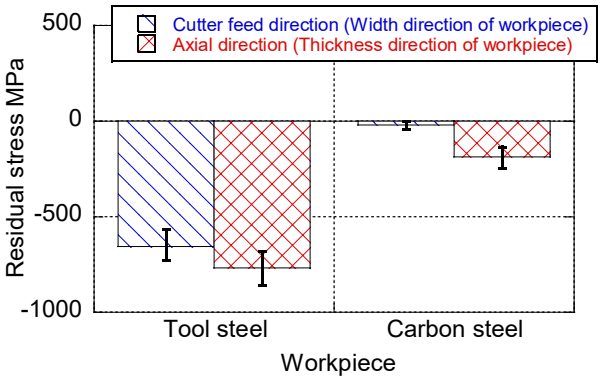

Fig. 3 Residual stresses in subsrface.

Cutting Force in Milling of Cold Work Tool Steel

Figure 2 compares the measured cutting forces in milling of tool steel and carbon steel at a cutting speed of 25 m/min and a feed rate of 0.05 mm/tooth. The cutting force changes periodically in 0.75 s of the tool rotation cycle. Since the cutting area of the helical end mill changes with the cutter rotation, the cutting force changes as:

1) the lowest point on the edge penetrates the bottom of the workpiece plate at O;
2) cutting force increases with the cutting area in O−A;
3) the cutting area moves upward and the cutting force becomes constant without changing the cutting area in A−B;
4) the cutting force decreases in B−C with the cutting area after the cutting edge exits from the top of the workpiece plate.

The large cutting force in milling of tool steel is confirmed because of the higher hardness, where the X and Y components of tool steel are 1.5 and 3.9 times larger than those of carbon steel. The Y component becomes significantly large in comparison to the X component in milling of tool steel. It suggests that the indentation effect of the edge radius is greater than that in milling of carbon steel, as described later.

Materials Research Proceedings 28 (2023) 1295-1302 https://doi.org/10.21741/9781644902479-140

Surface Finish and Residual Stress

Fig. 3 shows the residual stresses of tool steel and carbon steel, where the positive value is estimated as tensile. The compressive residual stress of tool steel is much larger than that of carbon steel. The surface finishes and the height distributions were observed with a laser microscope (Keyence, VK9700), as shown in Fig. 4. The relatively better surface was obtained in milling of tool steel, as shown in Fig. 4(a), even though chatter marks are slightly left on the finished surface. Regarding the height distributions of the surface finishes, as shown in Fig. 4(b) and (d), the height differences are 9 and 20 μm tool steel and carbon steel, respectively. The built-up edge may overcut the workpiece in milling of carbon steel.

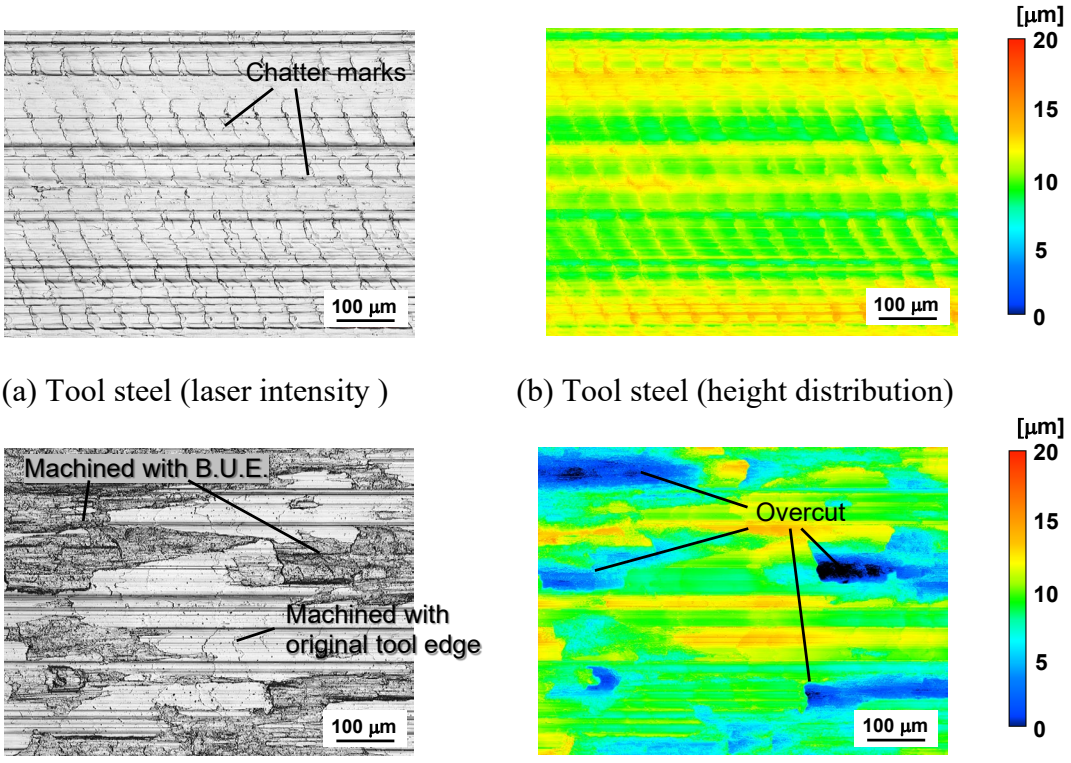

(a) Tool steel (laser intensity) (b) Tool steel (height distribution)

(c) Carbon steel (laser intensity) (d) Carbon steel (height distribution)

Fig. 4 Surface finishes.

Analytical Force Model in Milling

A force model is applied to characterize the cutting process in peripheral milling of tool steel. The force model in milling was presented in Reference [7]. The force model is briefly described here. A three-dimensional chip flow in milling is interpreted as a piling up of the orthogonal cuttings in the planes containing the cutting velocities V and the chip flow velocities V_c, as shown in Fig. 5. Although plastic deformation occurs in the chip formation, the interaction between each orthogonal cutting plane is ignored on the assumption that a rigid chip flows at an angular velocity. The orthogonal cutting models are given by the following equations:

$$\left.\begin{aligned}\phi &= \exp(A_{00}V + A_{01}t_1 + A_{02}\alpha + A_{03})\\ \tau_s &= \exp(A_{10}V + A_{11}t_1 + A_{12}\alpha + A_{13})\\ \beta &= \exp(A_{20}V + A_{21}t_1 + A_{22}\alpha + A_{23})\end{aligned}\right\} \quad (1)$$

Materials Research Proceedings 28 (2023) 1295-1302 https://doi.org/10.21741/9781644902479-140

where ϕ, τ_s and β are the shear angle, the shear stress on the shear plane, and the friction angle. V, t_1 and α are the rake angle, the cutting velocity, and the uncut chip thickness in the orthogonal cutting. A_{ij} (i = 0,1,2; j=0,1,2,3) are parameters acquired in the orthogonal cutting tests. The data can also be identified or refined with referring to the actual cutting force in milling by inverse analysis [8]. The cutting force should be regarded as the sum of the indentation force component due to the ploughing and the chip generation force component due to shearing in the shear zone and friction on the rake face. For the sake of simplicity, this study employs the orthogonal cutting data expressed as Eq. (1) on the assumption that the chip generation force component is the major effect here, where the indentation force component is implicitly associated with the parameters for the uncut chip thickness. Regarding friction on the rake face, the friction angle associated with the friction coefficient is controlled by the third equation in Eq. (1). Because the orthogonal cutting data are acquired in the actual cutting tests for the combination of the tool and the workpiece materials, friction in the interface between the tool face and the chip is characterized in the actual cutting. The shear angle and the shear stress on the shear plane depend on the material behavior. The thermal effect on the material behavior may be mainly controlled by the first term related to cutting velocity dependency, which is associated with the cutting temperature. Because the cutting energy is consumed into the shear energy in the shear plane and the friction energy on the rake face, the cutting energy is estimated in the chip flow model consisting of the orthogonal cuttings. Because the cutting energy depends on the chip flow direction, the chip flow angle is determined to minimize the cutting energy. Therefore, the cutting force is predicted in the determined chip flow model.

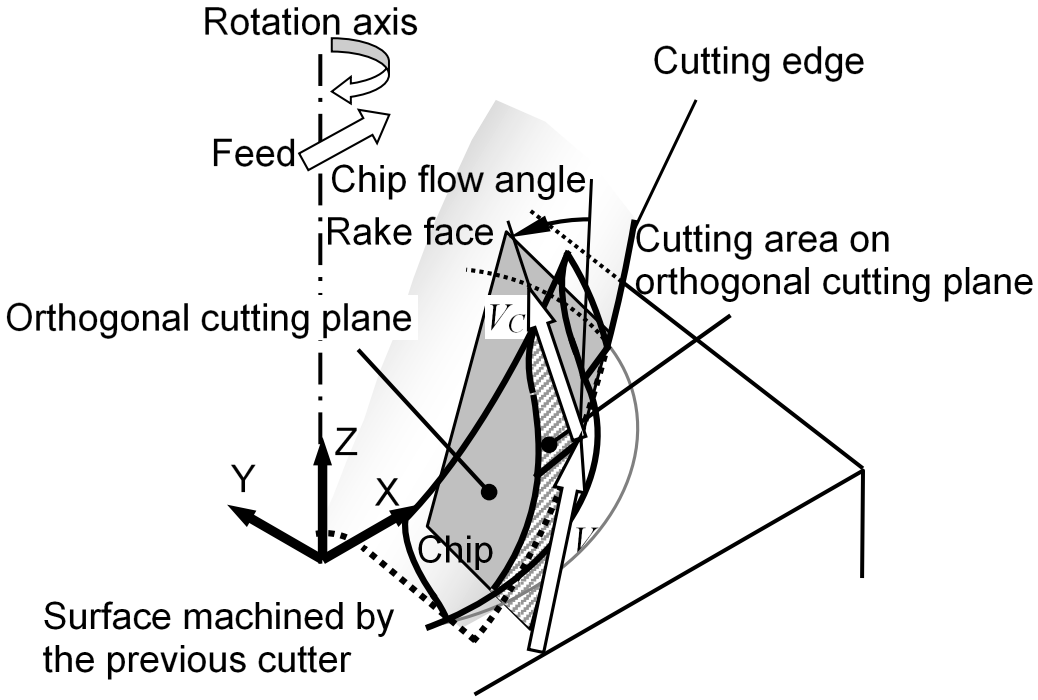

Fig. 5 Chip flow model in analysis.

Materials Research Proceedings 28 (2023) 1295-1302 https://doi.org/10.21741/9781644902479-140

Cutting Model in Cold Work Tool Steel

Based on the results of the cutting tests, the orthogonal cutting data were acquired as:
Tool steel:

$$\left.\begin{aligned}\phi &= \exp(0.189V + 34380t_1 - 6.781\alpha - 0.429)\\ \tau_s &= \exp(0.046V - 2172t_1 + 0.002\alpha + 21.25)\\ \beta &= \exp(-0.095V - 27280t_1 + 1.795\alpha + 0.1696)\end{aligned}\right\} \quad (2)$$

Carbon steel:

$$\left.\begin{aligned}\phi &= \exp(0.254V - 11450t_1 + 0.487\alpha - 3.037)\\ \tau_s &= \exp(-0.001V - 2121t_1 + 0.009\alpha + 20.10)\\ \beta &= \exp(-0.042V - 5414t_1 - 1.357\alpha - 0.266)\end{aligned}\right\} \quad (3)$$

Figure 6 compares the simulated and the measured cutting forces at the same cutting conditions in Fig. 2. The force model and the orthogonal cutting data are verified in the agreement of the

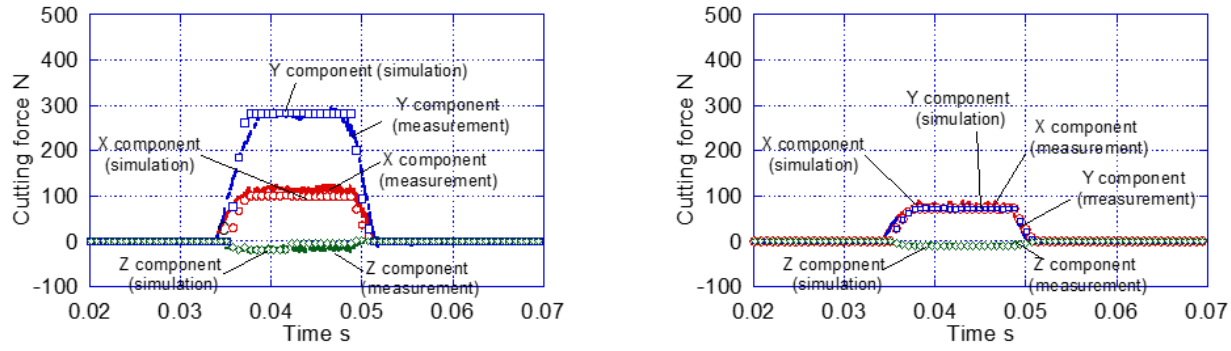

(a) Tool steel (b) Carbon steel

Fig. 6 Cutting force simulations.

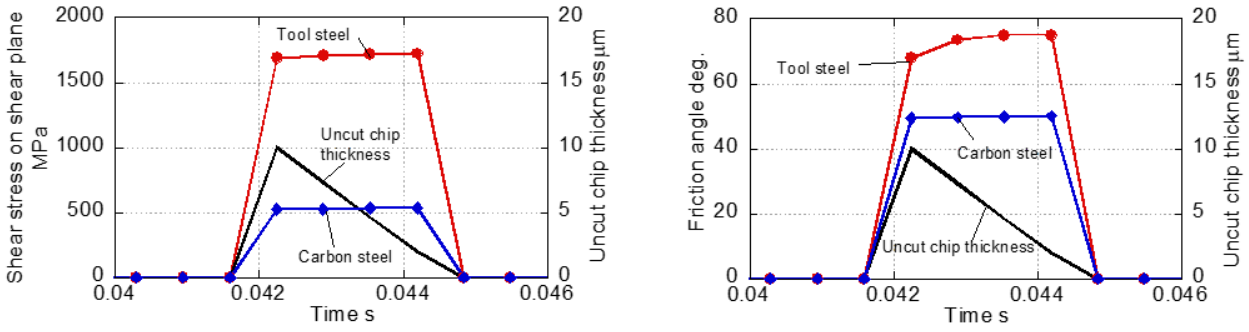

(a) Shear stress on shear plane (b) Friction angle

Fig. 7 Changes in cutting models at a center of axial depth of cut.

simulated cutting force with the measured force. Figure 7 shows the change in shear stress on the shear plane and the friction angle at the center of the plate thickness of the workpiece, where the uncut chip thickness is also shown as a reference. The uncut chip thickness decreases with the cutter rotation in down-cut process. The shear stress on the shear plane in milling of tool steel reaches about 3.3 times larger than that of carbon steel. The shear stresses of both materials are

nearly constant for the change in the uncut chip thickness. Then, the friction angle of tool steel becomes about 1.4 times larger than that of carbon steel at the edge engagement and increases with decreasing the uncut chip thickness. Meanwhile, the friction angle of carbon steel does not increase significantly. Since the coefficients in the second terms of uncut chip thickness in friction angle in equations (2) and (3) involve the indentation effect of the edge radius, the result shows that the indentation effect of the cutting edge in milling of tool steel is relatively much larger than that of carbon steel. Burnishing on the interface between the finished surface and the cutting edge promotes the compressive residual stress in subsurface [9]. Therefore, in milling of tool steel, a large compressive residual stress is induced by burnishing with a large indentation force on the edge radius. On the other hand, the original tool edge does not finish the machined surface and does not promote the burnishing effect on the machined surface in milling of carbon steel, because the built-up edge generates the overcut surface, as shown in Fig. 4(d). The compressive residual stress in subsurface of carbon steel is not expected with less burnishing.

Summary

The paper has been studied the peripheral milling of hardened cold work tool steel to characterize the cutting process. The results are summarized as:

1) In milling of tool steel, the cutting force components in the feed and radial directions of the tool are 1.5 and 3.9 times greater than those of carbon steel.
2) According to the analytical cutting simulation, the shear stress on the shear plane and the friction angle of tool steel becomes much larger than that of carbon steel. Because of the large negative terms of uncut chip thickness in friction angle, the indentation effect of the cutting edge in milling of tool steel is larger than that of carbon steel
3) The large indentation force on the edge radius enhances burnishing to induce a large compressive residual stress in milling of tool steel. In contrast, the original tool edge does not finish the machined surface and does not promote the effect of burnishing on the machined surface in milling of carbon steel, because the built-up edge generates the overcut surface. As consequence, the effect of burnishing is small in milling of carbon steel.

References

[1] V.F.C. Sousa, F.J.G. Silva, Recent advances on coated milling tool technology-a comprehensive review, Coatings, 10 (2020), 3, https://doi: 10.3390/coatings10030235

[2] M.N. Durakbasa, A. Akdogan, A.S. Vanli, and A.G. Bulutsuz, Optimization of end milling parameters and determination of the effects of edge profile for high surface quality of AISI H13 steel by using precise and fast measurements, Measurement 68 (2015) 92-99, https://doi: 10.1016/j.measurement.2015.02.042

[3] A. Aramcharoen, P.T. Mativenga, S. Yang, K.E. Cooke, and D.G. Teer, Evaluation and selection of hard coatings for micro milling of hardened tool steel, Int J Mach Tools Manuf. 48 (2008), 14, 1578–1584, http://doi: 10.1016/j.ijmachtools.2008.05.011

[4] B. Denkena, J. Köhler, and B. Bergmann, Development of cutting edge geometries for hard milling operations, CIRP J Manuf Sci Technol, 8 (2015), 43-52, https://doi: 10.1016/j.cirpj.2014.10.002

[5] S. Caruso, D. Umbrello, J.C. Outeiro, L. Filice, and F. Micari, An experimental investigation of residual stresses in hard machining of AISI 52100 steel, Procedia Engineering, 19 (2011), 67-72. https://doi: 10.1016/j.proeng.2011.11.081

[6] M. Matsuda, K. Okita, T. Nakagawa, and T. Sasaki, Application of X-ray stress measurement for residual stress analysis by inherent strain method - Comparison of cosα and sin2Ψ method-, Mechanical Engineering Journal, 4 (2017), 5, 17-00022-17–00022, https://doi: 10.1299/mej.17-00022

[7] T. Matsumura and E. Usui, Predictive cutting force model in complex-shaped end milling based on minimum cutting energy, Int J Mach Tools Manuf, 50 (2010), 5, 458-466, https://doi: 10.1016/j.ijmachtools.2010.01.008
[8] T. Matsumura, T. Shirakashi, and E. Usui, Adaptive cutting force prediction in milling processes, International Journal of Automation Technology, 4(2010), 3, 221-228, https://doi: doi.org/10.20965/ijat.2010.p0221
[9] H. Mizutani and M. Wakabayashi, Influence of cutting edge shape on residual stresses of cut surface (Effects of rake angle and contact width of flank face), Transactions of the Japan society of mechanical engineers. C, 72 (2006), 715, 247-251